PHYSICAL REVIEW B VOLUME 24, NUMBER 4 15 AUGUST 1981

Surface states on Si(111)-(2×1)

F. J. Himpsel, P. Heimann, and D. E. Eastman
IBM Thomas J. Watson Research Center, Yorktown Heights, New York 10598
(Received 9 March 1981)

Surface-state energy bands for a single-domain Si(111)-(2×1) surface have been studied with angle-resolved photoemission using synchrotron radiation. From the angular photoelectron distributions seen with a display-type spectrometer, we conclude that there are two surface states near the top of the valence bands E_v, one at $E_v - 0.7$ eV around $\bar{\Gamma}$ [0.65 eV full width half maximum (FWHM)] and a second at $E_v - 0.15$ eV (0.4 eV FWHM) along the line $\bar{J}\bar{K}$. These states are found to be nearly dispersionless along the symmetry lines $\bar{\Gamma}\bar{J}'$ and $\bar{J}\bar{K}$. Their range of existence can be related to different gaps in the projected bulk bands. The lower surface state lies in a band gap above the L_3 point which we find at $E_v - 1.5$ eV. Our findings are not well described by band calculations reported to date which use buckled-surface model geometries. Our results also indicate that several discrepancies among different reported experimental results are likely due to multidomain cleavage effects. We conclude that either the geometry of Si(111)-(2×1) has not yet been determined unambiguously or that the surface states cannot be described by a bandlike model which is the basis of present calculations.

INTRODUCTION

The cleaved Si(111)-(2×1) surface has been studied quite extensively using low-energy electron diffraction (LEED), angle-resolved photoemission, etc., and is widely believed to have a buckled-surface (2×1) geometry in which alternate rows of surface atoms are raised and lowered (e.g., see discussion and references in Ref. 1). Experimentally, there have been difficulties in preparing single-domain cleavages with reproducible photoemission features,[2-6] e.g., peak positions can vary up to ~0.5 eV (Ref. 3) and the amount of band dispersion measured along $\bar{\Gamma}\bar{J}'$ has varied from 0.5 eV (Ref. 3) to <0.1 eV (Ref. 5). Along $\bar{\Gamma}\bar{J}$ no band dispersion data have been reported. We have taken care to prepare single-domain Si(111)-(2×1) cleavage surfaces which are stable and reproducible, and have studied polarization-dependent surface-state bands throughout the surface Brillouin zone by using an imaging two-dimensional photoelectron spectrometer. We have measured surface-state dispersions $E(\vec{k}_{\parallel})$ along the main symmetry lines $\bar{\Gamma}\bar{J}'$ and $\bar{\Gamma}\bar{J}$. Also, we have measured the polarization dependence of surface-state emission, which yields symmetries. By exposing the (2×1) cleavage surface to activated H, the Si(111)-H(1×1) surface is formed, and differences in emission from these surfaces help distinguish bulk states from surface states. Our main result is that we find two distinguishable surface states near the top of the valence band which exist in different areas of the surface Brillouin zone and exhibit different sensitivities to hydrogen exposure. These states cannot be described in terms of calculated surface bands reported to date for buckled surface geometries.[7-10,13] Empirically, we locate the two surface states in two different band gaps of the projected bulk band structure. We conclude that either the geometry of Si(111)-(2×1) has not yet been determined unambiguously or that the surface states cannot be described by a bandlike model which is the basis of present calculations.

EXPERIMENTAL

The energy and angular distributions of photoelectrons from cleaved Si(111)-(2×1) and hydrogen-exposed Si(111)-H(1×1) have been measured with a two-dimensional photoelectron spectrometer[11] using synchrotron radiation from Tantalus I at the University of Wisconsin-Madison. Intrinsic p-type (boron-doped, 20 Ω cm) samples were cleaved in a vacuum of $\leq 10^{-10}$ Torr. Single-domain cleavages with low step density (i.e., no visible streaking of the LEED spots) were selected with LEED. For good-quality cleaves, the short symmetry direction $\bar{\Gamma}\bar{J}'$ of the surface Brillouin zone was parallel to the cleavage direction. All electron energies have been measured with respect to the Fermi level E_F which was determined from the Fermi edge of the Ta sample holder. However, we reference the energies to the top of the valence band E_v for better comparison with theory by using $E_F - E_v = 0.33$ eV for Si(111)-(2×1) (see Ref. 6). For Si(111)-H(1×1) we obtain $E_F - E_v = 0.46$ eV. For the data presented here, the electric field of the incident light was either polarized in the $\bar{\Gamma}\bar{J}'$ direction (s polarized) or mixed (s, p polarized) with the main components along $\bar{\Gamma}\bar{J}'$ and along the sample normal.

RESULTS

Figure 1 shows a set of angle-resolved photoelectron spectra at high-symmetry points of the

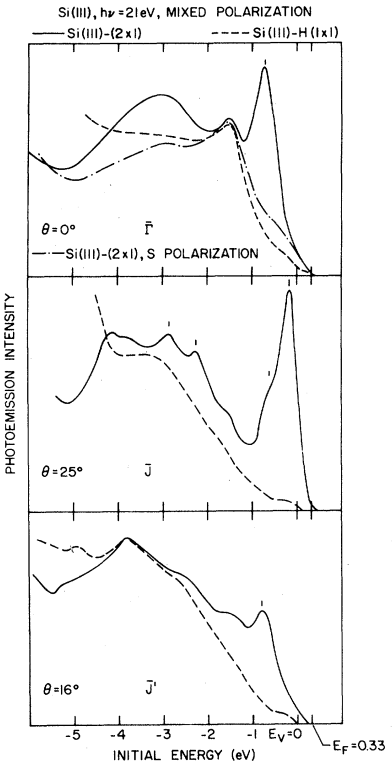

FIG. 1. Angle-resolved photoelectron spectra from a single-domain Si(111)-(2×1) surface (full lines and dashed-dotted line) and from Si(111)-H(1×1) (dashed lines) at $h\nu = 21.0$ eV. The escape angle θ from the sample normal and the azimuth have been chosen such that states near high-symmetry points of the surface Brillouin zone (see Fig. 4) are selected. Adsorbate-sensitive states are marked by tic marks.

(2×1) surface Brillouin zone. Spectra are shown for the clean Si(111)-(2×1) surface (full lines) and for Si(111)-H(1×1) (dashed lines). The dominant adsorbate-sensitive structures are tic-marked.

For $\vec{k}_{\parallel} = 0(\bar{\Gamma})$ there is a strong surface state at 0.7 eV below the valence-band maximum (strictly speaking, this is a surface resonance since it overlaps bulk bands). This corresponds to the dominant structure seen in previous angle-integrated and angle-resolved photoemission experiments.[2-5] There is a certain scatter in the reported values for the energy position of this surface state (relative to E_F our value of −1.03 eV compares to −1.15 eV in Ref. 2, about −0.6 eV in Ref. 3, −1.05 eV in Ref. 4, and −0.85 eV in Ref. 5). This is much larger than the scatter that we observe between different cleavages (less than ±0.05 eV). This may be due to difficulties in determining the position of the Fermi level E_F. The surface state at $\bar{\Gamma}$ is not excited when s-polarized light ($\vec{E} \parallel \bar{\Gamma}\bar{J}'$, dash-dotted line) is used, i.e., it is only excited by the component of $\vec{E}$ perpendicular to the surface. Therefore, it is fully symmetric (A_1 symmetry) with respect to the symmetry group operations at $\bar{\Gamma}$, and corresponds to an s, p_z-type orbital. In addition to the state at −0.7 eV, we observe a broad surface resonance with A_1 symmetry at ~−3 eV. In contrast to a previous interpretation,[3] we find that the structure at −1.5 eV at $\bar{\Gamma}$ is due to a bulk band. This feature is not sensitive to H exposure (see Fig. 1) and disperses with varying photon energy $h\nu$ (Fig. 2) in contrast to the surface state at −0.7 eV. For this feature the symmetry of the initial-state band is Λ_3 ($p_{x,y}$ type) since it is excited by the component of $\vec{E}$ parallel to the surface (see Fig. 1, s polarization). At $h\nu = 21$ eV, in particular, one is at the bulk L point (to be discussed) which leads us to assign the structure at −1.5 eV to the L_3' point.

Near $\bar{J}$ [Fig. 1, middle panel; see Fig. 4 for (2×1) surface Brillouin-zone symmetry point labels] we find a dominant surface state at −0.15 eV, as well as a remnant of the above-mentioned −0.7 eV state. Two weak surface resonances appear around $\bar{J}$ at −2.25 and −2.85 eV.

Near $\bar{J}'$ (Fig. 1, bottom panel) the predominant surface state at −0.7 eV is seen with decreased intensity and the −0.15-eV state is not seen. The structure at −3.9 eV is due to bulk interband transitions.

Following the dispersion of various surface states with $\vec{k}_{\parallel}$ (Figs. 3 and 4), we find a very slight (downwards) dispersion of the dominant −0.7-eV surface state along $\bar{\Gamma}\bar{J}'$. This is consistent with Ref. 5 but in contrast to the results of Ref. 3 where an upwards dispersion of 0.5 eV was found. We also studied cleavages with multidomain LEED patterns as reported in Ref. 3. In this case the

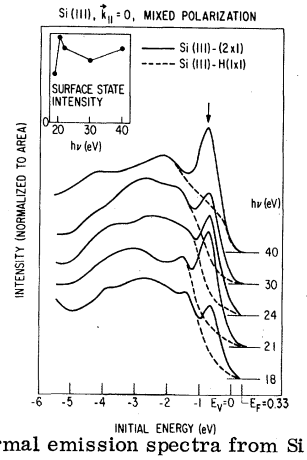

FIG. 2. Normal emission spectra from Si(111)-(2×1) and Si(111)-H(1×1) for various photon energies in mixed s,p polarization. The inset shows the surface-state cross section relative to the bulk taken from difference spectra.

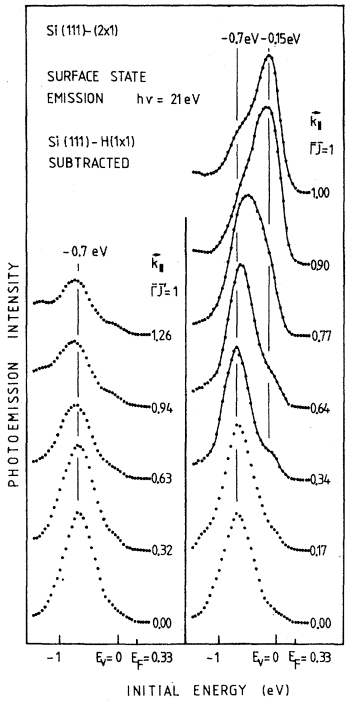

FIG. 3. Angle-resolved difference spectra between Si(111)-(2×1) and Si(111)-H(1×1) along the main symmetry lines $\overline{\Gamma J}$ and $\overline{\Gamma J'}$ showing the emission due to surface states near the top of the valence band.

upper surface state appears in several escape directions and an upwards dispersion in the $\overline{\Gamma J}'$ direction was sometimes observed. We explain this by the presence of additional (2×1) domains where the $\overline{\Gamma K}$ lines of additional domains are projected onto the $\overline{\Gamma J}'$ line of the first domain.

Along $\overline{\Gamma J}$ we find that the dominant surface-state peak stays constant at −0.7 eV up to ~0.7 $\overline{\Gamma J}$ and appears to disperse rapidly towards −0.15 eV beyond that point. We cannot rule out such an assignment but our data indicate that this rapid peak shift with $\bar{k}_\parallel$ is better described by the appearance of a new surface state near $\bar{J}$ than by a dispersion of a surface state band along $\overline{\Gamma J}$. This is substantiated by the angular distributions of the photoemission intensity at a given energy measured with the imaging two-dimensional spectrometer (Fig. 5). At $E_i = -0.7$ eV (relative to the top of the valence band), the emission is mainly concentrated in the interior of the surface-Brillouin zone. At $E_i = +0.1$ eV, only the zone boundary line $\overline{JK}$ contributes. At an intermediate energy $E_i = -0.4$ eV, these two areas of surface-state emission coexist and form separate emission patterns centered around 0.4 $\overline{\Gamma J}$ and 0.7 $\overline{\Gamma K}$, respectively. Therefore, we assign two separate sur-

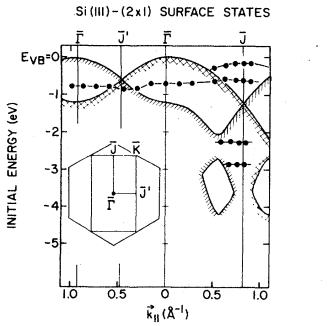

FIG. 4. Experimental energy bands of surface states for Si(111)-(2×1). The projection of bulk bands is shown by dashed areas. Two sets of projected bulk bands are shown which correspond to the two (2×1) Brillouin zones shown in Fig. 6. The main surface states at −0.7 and −0.15 eV are found in the two different gaps of the projected bulk bands.

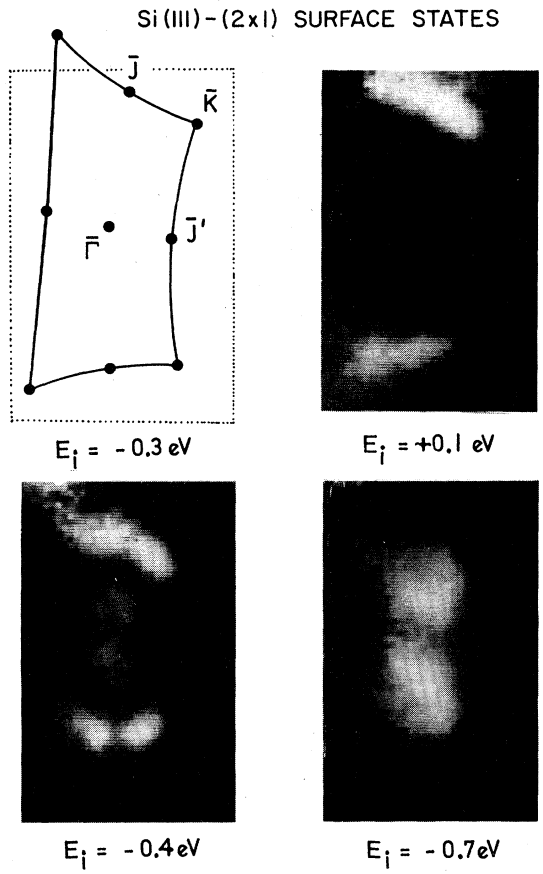

FIG. 5. Angular distribution of photoelectrons from the dominant Si(111)-(2×1) surface states as viewed on the screen of a two-dimensional spectrometer (Ref. 11) with mixed polarized light (see experimental section). For comparison, the projection of the surface Brillouin zone onto the screen is shown in a separate panel. There are two surface-state bands, one around $E_i = -0.7$ eV (relative to the top of the valence band), which exists in two lobes within the Brillouin zone, and the second near $E_i = -0.15$ eV which exists in the region around the zone boundary $\overline{JK}$.

face states to the data along $\overline{\Gamma J}$. This is further confirmed by hydrogen exposure in the submonolayer range (not shown here) which quenches the lower −0.7 eV surface state much more rapidly than the upper surface state.

DISCUSSION

The existence of the two predominant surface states can be understood in terms of the projected bulk bands (shown in Fig. 4 by dashed areas, from Pandey, private communication) if one takes the surface reconstruction into account. Near the top of the valence band there are two sets of projected bulk bands and the surface states exist in gaps above these projected bulk bands. One set of projected bulk bands (double hatched in Fig. 4) are those as given for an unreconstructed 1×1 surface; these show a maximum gap opening up near the zone boundary $\overline{J}$ where the upper surface state has maximum intensity (see Figs. 3 and 5). The second set of projected bulk bands (single hatched in Fig. 4) originates from surface umklapp due to the 2×1 reconstruction, which folds states near the zone boundary of the 1×1 Brillouin zone into the zone center of the 2×1 Brillouin zone via a surface momentum vector $\vec{g}$ as demonstrated in Fig. 6. The range in $\vec{k}$ space for the two surface states coincides with gaps in these two sets of projected bulk bands (Fig. 4). The lower surface state is located in a gap of the second set of projected bulk bands and has maximum intensity near the middle of the line $\overline{\Gamma J}$ (see Fig. 5) where the gap is largest (see Fig. 4). The minimum in the intensity of the lower surface state lies around $\overline{J'}$ (see Figs. 3 and 5) where this state barely overlaps with bulk bands (see Fig. 4).

Additional evidence for relating the two main surface states to bulk band gaps is given by the photon-energy-dependent cross section of the surface states (see Fig. 2 inset). As shown in Ref. 12, there are periodic oscillations in this cross section with maxima in the cross section at photon energies $h\nu_{max}$ such that final states are reached which have the same (three dimensional) $\vec{k}$ vector as the bulk states which span the gap. For normal emission from Si(111)-(2×1), the two bulk band gaps shown in Fig. 4 are terminated by the top of the valence band ($\Gamma'_{25}=0$ eV) and by the point $L'_3 = -1.5$ eV (−1.2 eV calculated), respectively. Taking a free-electron final band (inner potential of 19 eV below the vacuum level) one finds L points at +21 and +83 eV and an Γ point at +48 eV (above the top of the valence band) along the sample normal. Experimentally, one observes maxima in the cross section of the surface state at −0.7 eV in normal emission for $h\nu=21$ eV (see Fig. 2 insert and Ref. 4) and for $h\nu=48$ eV (Ref. 5). The maximum at $h\nu=21$ eV correlates to the band gap above the L'_3 point. Thus, the lower surface state appears to be split off from the lower lying set of projected bulk bands (single hatched, see Fig. 4). This can explain why this state seems not be affected by the underlying bulk bands.

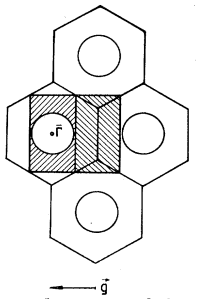

FIG. 6. Schematic explanation of the range of existence in $\vec{k}$ space for surface states on Si(111)-(2×1). The hatched areas represent gaps in the projected bulk bands at an average surface state energy of −0.4 eV (relative to the top of the valence band). The two rectangular 2×1 surface Brillouin zones cover the area of one hexagonal 1×1 surface Brillouin zone and support two different surface states. The $\vec{g}$ is the extra surface momentum vector induced by the (2×1) reconstruction.

Previous data on Si(111)-(2×1) have been compared rather favorably to band calculations (Refs. 3, 4, and 10). We do not find such an agreement for our new data which show differences with past data that we have discussed. There is a number of calculated surface-state bands for Haneman-type buckled surface geometry models[7-10,13] of the Si(111)-(2×1) surface which can be compared with our experimental surface-state bands. Common trends in these calculations are (a) an s,p_z dangling-bond-type surface-state band very near E_v which disperses upwards by about ~0.3 eV from $\overline{\Gamma}$ to $\overline{J'}$ and downwards from $\overline{\Gamma}$ to $\overline{J}$, and (b) back-bonds which are present for large buckling. The latter can be pushed up to within 0.5 eV of E_v by the reconstruction[7-10] and disperse more strongly ($\gtrsim 1$ eV) than the dangling-bond state. There are two possibilities to assign our observed surface states to calculated surface-state bands. First, all surface states could be assigned to a single dangling-bond-type surface-state band. Secondly, the surface states at −0.15 eV along $\overline{JK}$ and at −0.7 eV around $\overline{\Gamma}$ could be assigned to the dangling-bond and back-bond states, respectively.

However, there are several features in our data which do not agree with such assignments. Considering the first assignment, all band calculations except Ref. 9 conclude that the dangling-bond band disperses upwards from $\overline{\Gamma}$ to $\overline{J'}$ and has a maximum energy on the *short* surface Brillouin-zone boundary near $\overline{J'}$. In contrast (Figs. 3 and 4), we observe very slight downwards dispersion

along $\bar{\Gamma}\bar{J}'$. None of the calculations (Refs. 7–10, 13) gives an upwards dispersion for the dangling-bond state from $\bar{\Gamma}$ to $\bar{J}$, which could explain the surface state at −0.15 eV. Considering the second assignment, band calculations find the top of the back-bond state to be near $\bar{\Gamma}$ and have antisymmetric character with respect to the $(\bar{1}10)$ mirror plane. In contrast, we find the state at −0.7 eV to have symmetric s, p_z character at $\bar{\Gamma}$ (see discussion of Fig. 1, top panel). Also we find very little dispersion for this state compared with calculations. Substantial back-bond character has been suggested (Refs. 2, 7, and 9) for the lower state because a threefold symmetry had been found for the emission pattern.[2] It is remarkable that our surface-state emission pattern reflects the twofold symmetry of the reconstructed surface Brillouin zone (see pictures in Fig. 5) and not the threefold pattern of the projected bulk Brillouin zone. The threefold pattern found in earlier experiments[2] could be due to a multidomain structure or to a different measurement configuration. Thus significant discrepancies with such an assignment of dangling-bond and back-bond states are observed.

In summary, our surface state observations suggest that one-electron band calculations with buckled-surface model geometries reported to data (Refs. 7–10, 13) do not appear to give a correct description of Si(111)-(2×1); this does not preclude all possible buckled-surface models. Furthermore, the surface states could be sufficiently localized in space to make a bandlike picture inapplicable. This would be consistent with the very weak dispersions which we observe as well as with the small ($\lesssim 1$ eV) calculated bandwidths for the (1×1) surface. Also, the large charge transfer of almost a full electron from the lowered to the raised atoms inferred from band calculations[14] appears to be inconsistent with the observed core-level shifts[15,16] which suggest the transfer of about 0.1 to 0.3 electron. Possibly, the small bandwidths (i.e., weak overlap) of the Si dangling-bond orbitals results in significant correlation effects which are not included in the usual one-electron band calculations.

It is interesting to compare our surface-state data on Si(111)-(2×1) with similar data from Si(111)-(7×7) and laser-annealed Si(111)-(1×1) (Refs. 17–21). For Si(111)-(7×7) and Si(111)-(1×1), we find two surface states at −0.4 and −1.3 eV (relative to the top of the valence band). The upper state is located near the center of the surface Brillouin zone and has s, p_z character.[17,18] This state has been identified[19] with the lower Si(111)-(2×1) surface state at −0.7 eV (relative to the top of the valence band) which has similar symmetry. However, the energies differ by 0.3 eV (relative to the top of the valence band E_v) and only the different band bending of the different Si(111) surfaces [$E_F - E_v = 0.33$ eV for Si(111)-(2×1) versus $E_F - E_v = 0.51$ eV (Ref. 15) for Si(111)-(7×7) and Si(111)-(1×1)] reduces this difference to 0.1 eV when the Fermi level is taken as reference.[19] The upper surface state we observe for Si(111)-(2×1) has no analog on the other Si(111) surfaces. Only Si(111)-(7×7) has a higher-lying surface state near the Fermi level. However, this state has a different location in $\vec{k}$ space, i.e., a sharp emission cone with $k_{\parallel}$ equal to one half of the (1×1) surface Brillouin-zone boundary.[20,21] Likewise, the strong surface state at −1.3 eV for the (7×7) and (1×1) surfaces has no analog on the (2×1) surface, except the bulk-L_3' point at −1.5 eV. Thus, there are substantial differences in the surface electronic structure of various Si(111) surfaces. This indicates significant differences in local bonding geometries for the (2×1) and (7×7) surfaces which perhaps can be understood in terms of different reconstruction mechanisms.[22]

ACKNOWLEDGMENTS

We would like to thank K. C. Pandey for providing the projected bulk bands and J. F. van der Veen for help with the data evaluation. Also, we acknowledge J. Donelon, A. Marx, and the staff of the Synchrotron Radiation Center (University of Wisconsin-Madison) for their assistance. This work has been supported in part by the Air Force Office of Scientific Research (AFOSR), United States Air Force, under Contract No. F49620-80-C0025.

[1] D. E. Eastman, J. Vac. Sci. Technol. 17, 492 (1980).
[2] J. E. Rowe, M. M. Traum, and N. V. Smith, Phys. Rev. Lett. 33, 1333 (1974); M. M. Traum, J. E. Rowe, and N. V. Smith, J. Vac. Sci. Technol. 12, 298 (1975).
[3] M. W. Parke, A. McKinley, and R. H. Williams, J. Phys. C 11, L993 (1978); A. W. Parke, *ibid.* 12, 2447 (1979).
[4] G. V. Hansson, R. Z. Bachrach, R. S. Bauer, D. J. Chadi, and W. Gopel, Surf. Sci. 99, 13 (1980).
[5] G. M. Guichar, F. Houzay, R. Pinchaux, and Y. Petroff, *Proceedings of the 15th International Conference on the Physics of Semiconductors, Kyoto, 1980*, J. Phys. Soc. Jpn. 49 (1980), Suppl. A, p. 1047.
[6] F. G. Allen and G. W. Gobeli, Phys. Rev. 127, 150

(1962); M. Erbudak and T. E. Fischer, Phys. Rev. Lett. 29, 732 (1972); C. Sebenne, D. Bolmont, D. Guichar, and M. Balkanski, Phys. Rev. B 12, 3280 (1975).
[7]K. C. Pandey and J. C. Phillips, Phys. Rev. Lett. 34, 1450 (1975).
[8]J. A. Appelbaum and D. R. Hamann, Phys. Rev. B 12, 1410 (1975).
[9]M. Schluter, J. R. Chelikowsky, S. G. Louie, and M. L. Cohen, Phys. Rev. B 12, 4200 (1975).
[10]S. Ciraci and I. P. Batra, Solid State Commun. 18, 1149 (1976).
[11]D. E. Eastman, J. J. Donelon, N. C. Hien, and F. J. Himpsel, Nucl. Instrum. Methods 172, 327 (1980).
[12]S. G. Louie, P. Thiry, R. Pinchaux, Y. Petroff, D. Chandesris, and I. Lecante, Phys. Rev. Lett. 44, 549 (1980).
[13]F. Casula and A. Selloni, Solid State Commun. 37, 495 (1981).
[14]D. J. Chadi, J. Vac. Sci. Technol., in press.
[15]F. J. Himpsel, P. Heimann, T.-C. Chiang, and D. E. Eastman, Phys. Rev. Lett. 45, 1112 (1980).
[16]S. Brennan, J. Stöhr, R. Jaeger, and J. E. Rowe, Phys. Rev. Lett. 45, 1414 (1980).
[17]D. E. Eastman, F. J. Himpsel, J. A. Knapp, and K. C. Pandey, *Physics of Semiconductors, 1979,* edited by B. H. Wilson (Institute of Physics, London, 1979), Vol. 43, p. 1059.
[18]F. Houzay, G. M. Guichar, R. Pinchaux, P. Thiry, Y. Petroff, and D. Dagneaux, Surf. Sci. 99, 28 (1980).
[19]D. J. Chadi, R. S. Bauer, R. H. Williams, G. V. Hansson, R. Z. Bachrach, J. C. Mikkelsen, Jr., F. Howzry, G. M. Guichar, R. Pinchaux, and Y. Pétroff, Phys. Rev. Lett. 44, 799 (1980).
[20]G. V. Hansson, R. I. G. Uhrberg, and S. A. Flodström, Surf. Sci. 89, 159 (1979).
[21]F. J. Himpsel, D. E. Eastman, P. Heimann, B. Reihl, C. W. White, and D. M. Zehner, Phys. Rev. B 24, 1120 (1981); D. M. Zehner *et al.* (unpublished).
[22]D. J. Chadi, J. Vac. Sci. Technol. 17, 989 (1980).

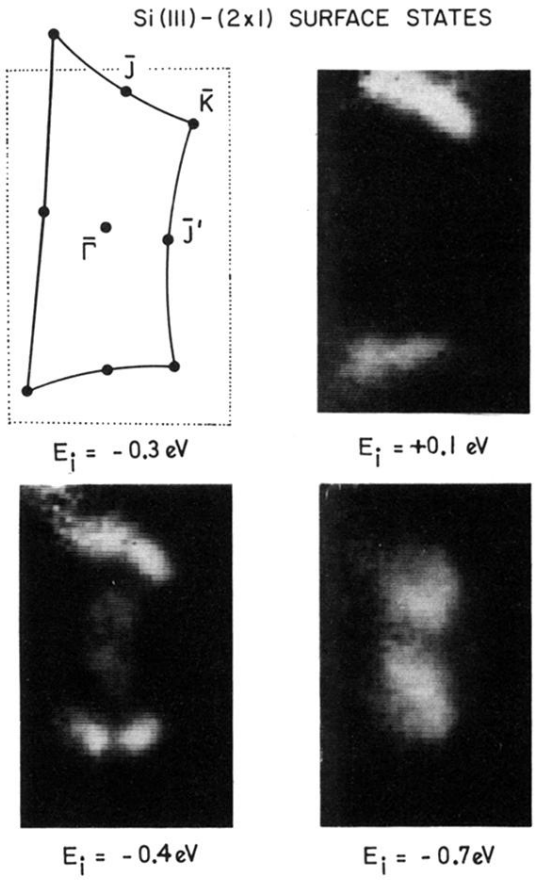

FIG. 5. Angular distribution of photoelectrons from the dominant Si(111)-(2×1) surface states as viewed on the screen of a two-dimensional spectrometer (Ref. 11) with mixed polarized light (see experimental section). For comparison, the projection of the surface Brillouin zone onto the screen is shown in a separate panel. There are two surface-state bands, one around $E_i = -0.7$ eV (relative to the top of the valence band), which exists in two lobes within the Brillouin zone, and the second near $E_i = -0.15$ eV which exists in the region around the zone boundary $\overline{JK}$.